치의과학 박사 학위논문

Three-dimensional finite element analysis of mandibular distal extension implant-assisted removable partial denture

하악 후방연장 임플란트-보조 가철성 국소의치의 삼차원 유한요소분석

2018 년 8 월

서울대학교 대학원

치의과학과 치과보철학 전공

엄 주 원

-ABSTRACT-

Three-dimensional finite element analysis of mandibular distal extension implant-assisted removable partial denture

Ju-won Eom, *D.D.S., M.S.D.*
Department of Prosthodontics,
Graduate School, Seoul National University.
(Directed by Prof. ***Ho-Beom Kwon****, DDS, MSD, Ph.D.)*

Purpose : The purpose of this study was to assess the possibility of implant-supported fixed prostheses as RPD abutments using 3D-finite element analysis.

Materials and methods : Finite element models of the mandible and teeth were generated based on a patient's computed tomography (CT) data. The teeth, surveyed crowns, RPDs and IARPDs were created in the model using 3D software. With the generated components, three types of 3-dimensional finite element models of bilateral mandible were constructed: tooth-tissue-supported RPD with four abutment teeth (4TT), implant-tissue-supported RPD with four implants (4IT), implant-tissue-supported RPD with two implants (2IT).

Oblique force was directed at 11.54 degrees to the long axis of the crown from the buccal to the lingual direction and distributed to the central fossa and the lingual slopes of the buccal cusps of all maxillary premolars and molars in the models. Finite element analysis was performed with software (ANSYS 14.5; Swanson Analysis Systems, Inc). The biomechanical behaviors of the models were analyzed by comparing von Mises stresses and displacements of the models.

Results : The highest von Mises stress value among the three models was 242.2 MPa and occurred in model 4TT. The highest von Mises stress value of model 4IT was slightly greater than that of model 2IT. The highest von Mises stress values in all three models were observed on the RPD framework. The second highest von Mises stress among the components of IARPDs occurred on the implant abutments. The highest von Mises stress value of the implant in model 4IT was slightly smaller than that in model 2IT.

The maximum displacement of the all three models appeared on the most distal acrylic resin base of RPDs. The maximum displacement value of model 4TT was the highest among the models, while the maximum displacement value in the RPD framework of model 4IT was the lowest. The displacement value of model 2IT was slightly larger than that of model 4IT.

Conclusion : The highest stress was concentrated on the RPD frameworks in all three types of RPDs, and that the difference between the highest von Mises stress values and the difference between the maximum displacement values of three models were not great. Although more considerations concerning about the RPD design and the number or location of the implant are needed, it was found that IARPDs in which the implants were used as RPD abutments could be one of the treatment modalities for the mandibular distal extension cases.

Key Words : Dental implant, Implant-assisted removable partial denture, Implant-supported removable partial denture, Three dimensional finite element analysis, Mandibular distal extension removable partial denture

Student Number : 2011-31182

CONTENTS

I. Introduction

Removable partial dentures (RPDs) with implants have been developed one of prosthetic treatment options for patients with partial edentulism. (Jang et al. 1998) Recently, implant-assisted removable partial dentures (IARPDs) are frequently used as an treatment option. (Mijiritsky 2007; Bae 2017) An IARPD are different from conventional RPDs, implant-retained RPD or implant-supported RPD in that implants are used as surveyed crowns for the RPD abutments, while implant are used as attachments in implant-retained RPD or implant-supported RPD. (Yeung et al. 2014; Wismeijeret al. 2013; Halterman et al. 1999; de Carvalho et al. 2001) The IARPDs have several advantages. The implants used as RPD abutments provide additional retention and support to improve masticatory efficiency, which provide comfort and satisfaction for patients. (Mijiritsky 2007) The implants in IARPDs could maintain the remaining bone. (Keltjens et al. 1993; Werbitt and Goldberg 1992) The clasp arm could be left out by retentive attachment of implant prosthesis, which would be more esthetic for patients. In addition, the IARPDs are very cost-effective, especially in Korea by national health insurance. (de Carvalho et al. 2001) Furthermore, transforming Kennedy class I RPD to Kennedy class III by placing distal implants, higher maximum bite force was given for the patients using IARPDs than conventional RPDs. (Ohkubo et al. 2008; Shahmiri and Atieh 2010)

In recent studies, partial mandibular edentulous patients were more satisfied with mandibular IARPDs than conventional RPDs in stability, chewing efficiency and appearance. (Wismeijer et al. 2013)

The implant used as a conventional abutment in IARPD showed more preferable results than the implant used as an attachment in overdenture type of RPD. The marginal bone loss of implant were higher in implant used as attachment than in implant used as conventional abutment, and there were more complications in the former implant than the latter implant. (Bae et al. 2017)

Finite element analysis is a frequently used tool in dentistry to analyze biomechanical behavior of prostheses. (Geng et al. 2001; Mericske-Stern et al. 1995; Baggi et al. 2008; Lang et al. 2003; Anitua et al. 2010; Murakami and Wakabayashi 2014) Although there have been many case reports about the RPDs in conjunction with implant prosthesis using 3D finite element analysis, there are few studies in which the implant prosthesis was used as abutments for the RPDs using 3D finite element analysis. Pellizzer et al. demonstrated the stress distribution between a distal extension RPD and different retentive attachments including an implant prosthesis used as an surveyed abutment. (Pellizzer et al. 2010). The author concluded that healing abutments, ERA attachments, and O'ring systems were viable with RPDs, but the single implant-supported prosthesis as an distal abutment for the Kennedy class III RPD was nonviable because single implant-supported prosthesis had a large displacement with oblique load. However, the study used 2D FEA and the individual components including the RPD components, the surveyed crown and the implant including a fixture, an abutment and a screw were not fully incorporated.

In a previous study, the biomechanical behavior of an implant crown, bone, and an IARPD in a partial maxilla 3D model, and compared stress distributions of implant fixtures as abutments in four different types of IARPDs with those of denture abutment tooth were analyzed by using 3D finite element analysis. (Eom et al. 2017) It was concluded that the highest stress was concentrated on the implants in both IARPDs in the study and because the stress from the occlusal loading was concentrated primarily on the implant when implants were used for the RPD abutments, more considerations concerning the RPD design and the number or location of the implant are necessary. However, the previous study was performed with only half of the maxilla and the partial RPD, and the contralateral side could have affected the results. Therefore, the purpose of this study was to assess the possibility of implant-supported fixed prostheses as RPD abutments using 3D-finite element analysis.

Ⅱ. Material and Methods

Finite element models of the mandible and teeth were generated based on a patient's computed tomography (CT) data. The teeth, surveyed crowns, RPDs and IARPDs were created in the model using 3D software. With the generated components, three 3-dimensional finite element models of bilateral mandible were constructed: tooth-tissue-supported RPD with four abutment teeth (4TT), implant-tissue-supported RPD with four implants (4IT), implant-tissue-supported RPD with two implants (2IT). Oblique loading of 300 N was applied on the crowns and denture teeth. The von Mises stress and displacement of the denture abutment tooth and the implant system were identified. Oblique loading of 300 N was exerted on the crown and the denture teeth to simulate masticatory loading. (O'Mahony et al. 2001; Mericske-Stern et al. 1995) The stress distribution and the displacement of implants, bone, teeth, a RPD and IARPDs were identified. This study was approved by the institutional review board of Seoul National University Dental Hospital.

The geometry of mandible was generated from a patient computed tomography (CT) data using the segmentation software (Amira, FEI), and then the geometry was exported into the meshing program (Visual-Mesh, ESI group), producing tetrahedral volumetric meshes of mandible. Three 3D finite element models representing mandible, abutments, and RPDs were constructed, and the mandible was composed of soft tissue, cortical bone and cancellous bone. The models were composed of mucosa, cortical bone and cancellous bone, periodontal ligaments, abutments, teeth, surveyed crown, implants and RPD. The surveyed crowns and the RPDs were fabricated in the CAD software(Visual-Mesh, ESI group) with the scan data of wax up of those on the artificial mandible model which was fabricated by three dimensional printing. The surveyed crown had rest seats and were modeled on the properties of zirconia. Each RPD had a lingual bar major connector, bilateral RPI clasps and canine extension rests.

A tooth-tissue-supported RPD model with four abutment teeth (4TT) consisted of 4 surveyed crowns supported by natural teeth in the area of the bilateral mandibular canines and premolars combined with a mandibular distal extension RPD. The mandible was created by removing the second premolar, and the first and second molar in the original model and by replacing the surveyed canine and the surveyed first premolar with the scan data of artificial teeth in the replica model (Nissin D50-555; Nissin).

An implant-tissue-supported RPD model with four implants (4IT) was identical to the model 4TT except that there were four implant supported fixed prostheses as the abutments for the IARPD in the area of the bilateral mandibular canines and premolars instead of natural teeth. An implant-tissue-supported RPD model with two implants (2IT) was identical to the model 4IT except that there were two implant supported fixed prostheses as the abutments for the IARPD in the area of the bilateral premolars and the surveyed crowns for the natural teeth were set in the area of the bilateral canines. The other anterior teeth were all natural teeth.

The geometries of the dental implant system including implant fixtures, abutments and abutment screws (Osstem GS system; Osstem Implant Co) provided by manufacturer were used. The dimension of the all implants was 10 mm in length, and 4 mm in diameter. The abutments and the abutment screws were assembled and a preload of 825 N was applied to them. (Lang et al. 2003) The abutment screws contacted with the implant screw hole. The inferior surface of the abutment contacted to the top of the implant. The preload simulating screw tightening was created by the bolt-pretension mechanism of the finite element analysis software ANSYS program. (ANSYS 14.5; Swanson Analysis Systems, Inc). (Montgomery 2002) The implant was considered to be bonded with cancellous and cortical bone to simulate complete osseointegration.
Meshes of teeth, surveyed crowns, and RPDs were created with 3D computer-aided design software (Visual-Mesh; ESI group) (Fig. 1).

The meshes for the roots of the teeth were surrounded by meshes of the periodontal ligament which was 0.2 mm in thickness. (Kojima et al. 2007) The RPD model was composed of a metal framework, acrylic resin base, and denture teeth. The acrylic resin base was considered to be completely bonded with the denture tooth and the metal framework. Nodes in the attachment areas of the masticatory muscles such as the masseter, the medial pterygoid, the lateral pterygoid, the temporal, and the suprahyoid muscles were fixed in all directions.

All materials were assumed to be linearly elastic, homogenous, and isotropic to simplify the calculations. The elastic modulus and the Poisson ratio for each material are summarized in Table 1.

Finite element analysis was performed with software (ANSYS 14.5; Swanson Analysis Systems, Inc). The interfaces between the surveyed zirconia crowns and the clasps of the RPDs were modeled as frictional contacts with appropriate friction coefficients (μ=0.13). (Keith et al. 1994) Contact analysis was also applied to the interfaces between implant components. The coefficient of friction value between the abutment and implant was 0.16, and that between the abutment and abutment screw was 0.2. (Shahmiri et al. 2014) Based on previous studies, oblique loading of 300 N was applied on the crown and denture tooth to simulate masticatory loading. (Budtz-Jorgensen et al. 2000; Keltjens et al. 1993) Oblique force was directed at 11.54 degrees to the long axis of the crown from the buccal to the lingual direction and distributed to the central fossa and the lingual slopes of the buccal cusps of all mandibular premolars and molars in the models (Fig. 2). (O'Mahony et al. 2001)

All nodes of the most medial and most distal surfaces in the models were constrained in all directions. The von Mises stress value was used for the analysis which are frequently used in predicting failure of success of dental materials such as titanium, cobalt-chromium, and zirconia. (Baggi et al. 2008) Higher value of von Mises stress could stand out for the higher risk of failure. (Geng et al. 2001; Van Staden et al. 2006; Himmlova et al. 2004) The von Mises stress values of the cortical bone, cancellous bone, RPD frameworks, and implants in natural teeth RPD and in the two different types of IARPDs were investigated. Maximum displacement values of the finite element model were calculated to verify which compartments in the models moved. All mechanical properties of the materials were based on the previous studies. (Geng et al. 2001; Lang et al. 2003; Murakami and Wakabayashi 2014; Shahmiri et al. 2013a)

Ⅲ. Results

The highest von Mises stress value among the three models occurred on 4TT. The highest von Mises stress value of model 4IT was slightly smaller than that of model 2IT. The highest von Mises stress values of the all three different types of RPDs occurred on the frameworks of the RPDs. The second highest von Mises stress values in the compartments of IARPDs occurred on the implant abutments. The maximum displacement was the greatest in model 4TT followed by 2IT,and 4IT sequentially. The maximum displacement of the all three models appeared on the most distal acrylic resin base of RPDs

The highest von Mises stress values of all models were observed in the framework of the each RPD (Table 2). The maximum von Mises stress value of the framework of the 4TT was greatest (Fig 3). With regard to the IARPDs, the highest von Mises stress value in model 4IT (228.1 MPa) was slightly greater than that in model 2IT (220.9MPa), which occurred on the framework of the IARPD (Table 3).

The highest von Mises stress value in the cortical bone on the cortical bone was 71.9 MPa, and occurred around the implant fixture of the model 2IT (Fig 4). The highest von Mises stress of cortical bone of model 4IT (66.5 MPa) was slightly less than the value of the model 2IT (71.9MPa). The highest von Mises stress of cortical bone in model 4TT (31.4 MPa) was less than half of the value in model 4IT (66.5MPa).

The highest von Mises stress of cancellous bone also occurred on the cancellous bone around the implant fixture of the model 2IT (2.7 MPa) (Fig 5). The highest von Mises stress value of cancellous bone in model 4IT (1.5 MPa) was almost half of the value in model 2IT (2.7 MPa). The highest von Mises stress value of cancellous bone in model 4TT (1.4 MPa) was slightly less than the value in model 4IT (1.5MPa).

The highest von Mises stress of the RPD framework occurred on the lowest part of proximal plate of the RPD frameworks (Fig 6). The maximum von Mises stress value of the RPD framework was greatest in model 4TT (242.2 MPa). The highest von Mises stress value of the RPD framework in model 4IT (228.1 MPa) was slightly greater than the value in model 2IT (220.9 MPa).

The highest von Mises stress value of the implant in model 4IT (214.8MPa) was slightly less than that in model 2IT (219.7MPa) (Fig 7). The highest von Mises stress of the implant in both model 4IT and 2IT occurred on the abutment of an implant in the area of mandibular second premolar.

The maximum displacement values of each model are listed in Table 4. The maximum displacements of the all three models appeared on the most distal flange of RPDs (Fig. 8). The maximum displacement value that occurred in the most distal acrylic base of the RPD of the model 4TT (0.2265 mm) was the highest among three models, while the maximum displacement value of model 4IT (0.2027 mm) was the lowest. The maximum displacement value of model 4IT was slightly less than that of model 2IT (0.2199 mm) (Table 4).

Ⅳ. Discussion

The purpose of this study was to assess that the implants could be used as surveyed crowns for the RPD abutments using 3D-finite element analysis to compare a conventional mandibular distal extension RPD with two types of IARPDs. The FEM analysis showed that the stress onto the conventional RPD was not much different from the stress onto the IARPDs. Because the maximum von Mises stress values of three model occurred at the similar area in the RPD framework, and the difference between the highest von Mises stress values and the maximum displacement values of three models were not great, it was concluded that the treatment with IARPDs could be used for the partial edentulism to ensure more retention and support.

As early as in 1993, Keltjens reported the RPD using implants. The author described that implants in conjunction with distal extension RPDs would prevent bone resorption beneath the denture base. It would provide additional retention for the RPD, reduce stress on the natural abutment teeth and the number of needed clasps for the RPD, and improve comfort for the patient. (Keltjens et al. 1993) Implant-supported fixed restorations could be used as abutments solely for RPDs. Jang et al. reported a case report using single implant-supported crown as an abutment for RPD. (Jang et al. 1998). It was reported that an implant was placed on the mandibular right canine area as an abutment to support the RPD for the patient who had only anterior teeth remaining in the mandible. After 14 months follow-up, the implant did not show any marginal bone loss, crown loosening, or pocket deepening. Ganz et al. placed two implants splinted with a bar attachment on the patient's maxilla. A removable partial denture which was retained and supported by natural surveyed crowns and bar was delivered to the patient. (Ganz 1991). Mitrani et al. reported a retrospective study of partially edentulous patients who had been placed implants on posterior region because of their unsatisfactory RPDs. The posterior implants provided retention and support of the RPDs, and eliminated the need for clasps which enhanced the esthetics. The result indicated that all patients showed increased satisfaction, and there is minimal component wear and no marginal bone loss around fixtures. (Mitrani et al. 2003)

Shahmiri et al. analyzed the mandibular distal extension IARPD by using finite element analysis. (Shahmiri et al. 2013b) Bilateral mandible model with an IARPDs were fabricated and the author analyzed the maximum deformation and the stress distribution of a framework and acrylic resin in the RPD, cortical or cancellous bone, and implants. The implants were located at the second molar regions and were associated with an RPD via ball attachment systems. The implant and abutment were regarded as a single solid structure. The deformation and elastic strain of the RPD framework were analyzed. The author concluded that the stress on the denture could make acrylic denture resin fracture, and the results were also similar to the present study results in that the highest strain in IARPD occurred on the framework.

The highest von Mises stress values in all three models were observed on the RPD frameworks, and it was assumed that the RPD framework had highest elastic modulus. (Shahmiri et al. 2013a) In the previous study (Eom et al. 2017), the highest von Mises stress occurred on the implants assumed to bear most of the loading of IARPDs in partially maxilla models. Meanwhile, the von Mises stress occurred on the frameworks of IARPDs in total mandible model of the present study. The contralateral parts of the RPD, teeth, and implants might have affected the different results from the previous study.

The highest von Mises stress value of the implant in model 4IT was slightly smaller than that in model 2IT. It was considered that the occlusal loading was distributed to the four implants which were less mobile than natural teeth with surveyed crowns. However, the difference of the values between two models was not much as the difference in number of the implants.

The natural tooth model (4TT) had the greater maximum displacement value than the implant models (4IT and 2IT). It was considered that the abutment teeth of the natural tooth RPDs were more displaceable than implants because of the periodontal ligament around the tooth root which had lower elastic modulus. The displacement of model 2IT was slightly larger than that of model 4IT. It could be explained by the total number of implants which were less mobile than natural abutment teeth. The displacement of both implant models was explained by the elasticity of the frameworks of the IARPDs.

The difference between the maximum displacement values of model 4TT, 4IT and 2IT in the present study was not much as the difference between those of the tooth-tissue-supported RPD and the implant-tissue-supported RPD in the previous study. (Eom et al. 2017) It was considered that the rigid bilateral major and minor connector, 4 RPD rest, 2 RPI clasp, and wider denture bearing area prevented the tissueward movements of the IARPDs.

As mentioned above, the difference of von Mises stress values of implants and the difference of displacement values between the two IARPD models were not much. It was assumed that the treatment option in which two implants were used as the abutments for the well-planned IARPD in model 2IT might have similar function and expectation to the treatment option in which four implants were used as the abutments for the IARPD in model 4IT.

Recently, patients over sixty five years old with partial edentulism are supported with two implants and a RPD with low treatment fee with Korean National Health Insurance system. An IARPD with two surveyed crown supported by implants could be a very cost-effective treatment option for the partial edentulous patients. Although the more number of implants used as the RPD abutment, the less the unfavorable force to the implants, two implants in an IARPD would be appropriate with well planned RPD design.

The contact force clamping the abutment and the implant fixture by screw elongation is called the preload. (Patterson and Johns 1992) The setting of implant preload could be modeled by applying torque value to the abutment screw using 3D modeled torque. (Lang et al. 2003). In this study, the 825 N of implant preload was formed by using the bolt-pretension mechanism which is included in the ANSYS program. (Montgomery 2002) In the previous study, (Lang et al. 2003) the 825 N preload was regarded as optimum preload to be the 75% of the yield strength as recommended for the implant-abutment assembled with a screw. Lang concurred that the 75% of the yield strength of the abutment screw would be equal as using a torque of 32 Ncm applied to the abutment screws with 0.12 of coefficient friction between the implant components.

In the present study, several assumptions were made that all materials in three models were homogenous, isotropic, and linearly elastic. Although the setting of contact condition between all interfaces was regarded as more real clinical situation than the setting of bonded condition, the contact analysis was adopted to the two interfaces. The first interface was between the implant components including implant fixtures, abutments and screws and the second interface was between the RPD framework and the surveyed crowns. All other interfaces except the two interfaces were set as bonded condition.

The displacement values of implants of IARPDs were no more than 25μm, which were within the normal range which is known as gradually reaching up to about 10 - 50 μm under lateral load (Kim et al. 2005). In addition, it was assumed that the IARPDs moved downward to the tissue on the occlusal load, and the tissue under the RPD base also resisted the occlusal load. It is recommended that the maximum support bearing area were needed in this case of IARPD to distribute the occlusal load to the denture bearing area. The reason of the different total deformation values between the implant model and natural tooth model was assumed that the abutment teeth of RPD associated natural tooth model were more mobile than those of RPD associated with implant model because of the periodontal ligament around the tooth root

It is necessary to consider much about the RPD design and the number or location of implants to use the implant as the surveyed crown same as the conventional RPD abutments. (Jang et al. 1998;

Pellecchia et al. 2000; Starr 2001) To protect the abutment tooth or the implant from the unfavorable force of lateral movements of the RPD, it is necessary to design clasps to allow the tissueward movement of the RPD. A RPI, a RPA, and a wrought wire clasp are frequently used for the distal extension RPD. In addition, the wrought wire clasps might be better to prevent the lateral force to the implant crown of the IARPD than the cast clasps, even though we used RPI clasps in this study to compare the models in the as much as same condition. (Frank et al. 1983)

As the conventional RPDs, the patients with IARPDs need periodic recall checks and have to reline the dentures in the resorbed edentulous area to prevent the occlusal loading from concentrating on the implants. (Bergman 1987; Bergman et al. 1982, 1995) Because the alveolar bone underneath the denture bearing area is gradually resorbed, the fitness of denture base becomes worse. Sequentially, the tissueward movement of RPD based on the fulcrum line gets greater, and the lateral force to the abutment tooth or implant via clasps or indirect retainer becomes greater. Therefore, the periodic recall check is very important to check the unfitted denture base due to the alveolar bone resorption. Whenever dentists find the unfitted IARPD, it should be relined immediately.

Ⅴ. Conclusion

Within the limitation of the present study, this three-dimensional finite element model analysis revealed that the highest stress was concentrated on the RPD frameworks in all three types of RPDs, and that the difference between the highest von Mises stress values and maximum displacement values of three models were not great. Although more considerations concerning about the RPD design and the number or location of the implant are needed, it was found that IARPDs in which the implants were used as RPD abutments could be one of the treatment modalities for the mandibular distal extension cases.

Table 1. Material properties of finite element models (Shahmiri et al. 2014; Wang et al. 2011)

Material	Elastic modulus (GPa)	Poisson ratio
Titanium	110	0.33
Acrylic resin	2.2	0.31
RPD framework (cobalt-chromium)	211	0.3
Tooth dentin	41	0.3
Gold alloy	91	0.33
Periodontal ligament (PDL)	3×10^{-5}	0.45
Cortical bone	13.7	0.3
Cancellous bone	1.37	0.33
MucosaZironia	210	0.27

Table 2. Highest von Mises stress values for each of finite element models

Model	4TT	4IT	2IT
von Mises stress value (MPa)	242.2`	228.1	220.9

Table 3. Highest von Mises stress values (MPa) in each compartment

Model	4TT	4IT	2IT
Cortical bone	31.4	66.5	71.8
Cancellous bone	1.4	1.5	2.7
RPD framework	242.2	228.1	220.9
Implant		214.8	219.7

Table 4. Highest maximum displacement value (mm) for each finite element model

Model	4TT	4IT	2IT
Maximum displacement	0.2265	0.2027	0.2199

Fig. 1. A, Occlusal view of models. B, Tooth-tissue-supported RPD model with four abutment teeth (4TT). C, Implant-tissue-supported RPD model with four implants (4IT). D, Implant-tissue-supported RPD model with two implants (2IT).

A

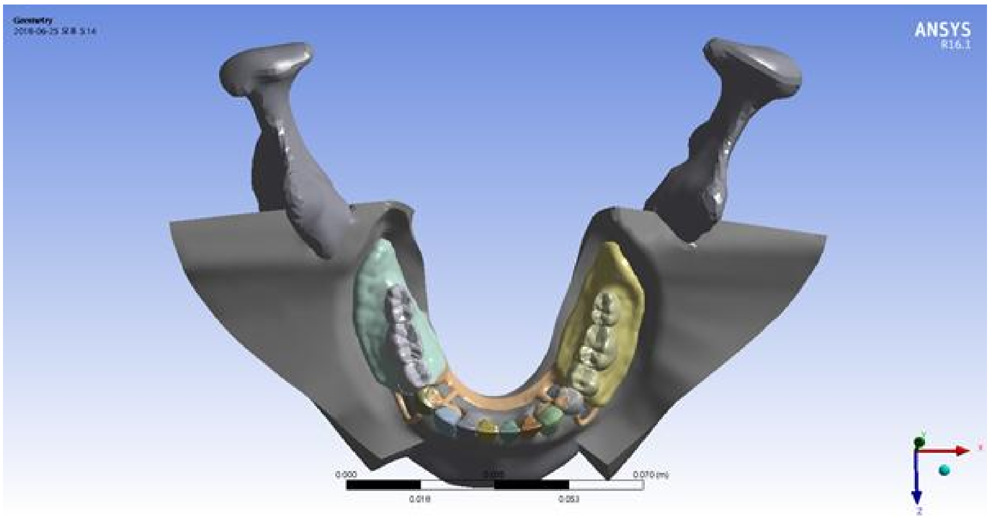

B

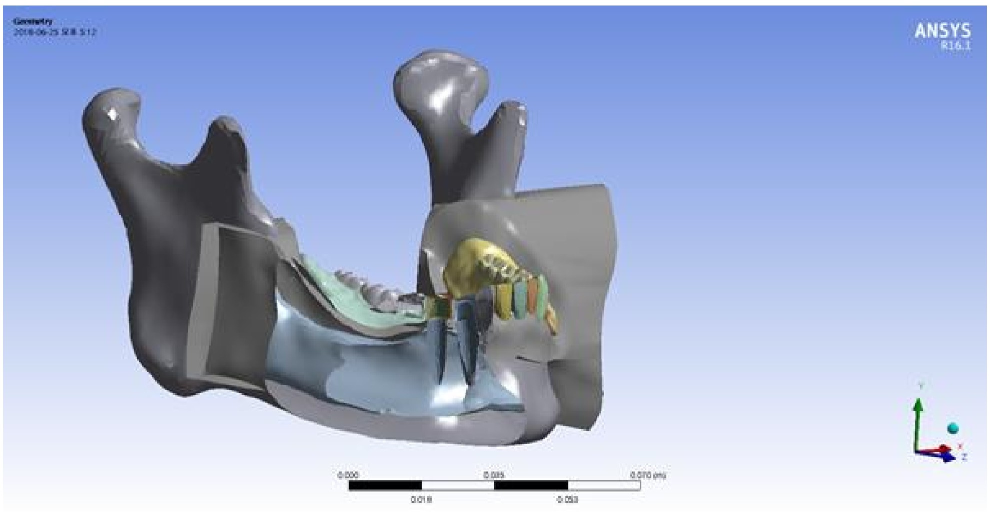

C

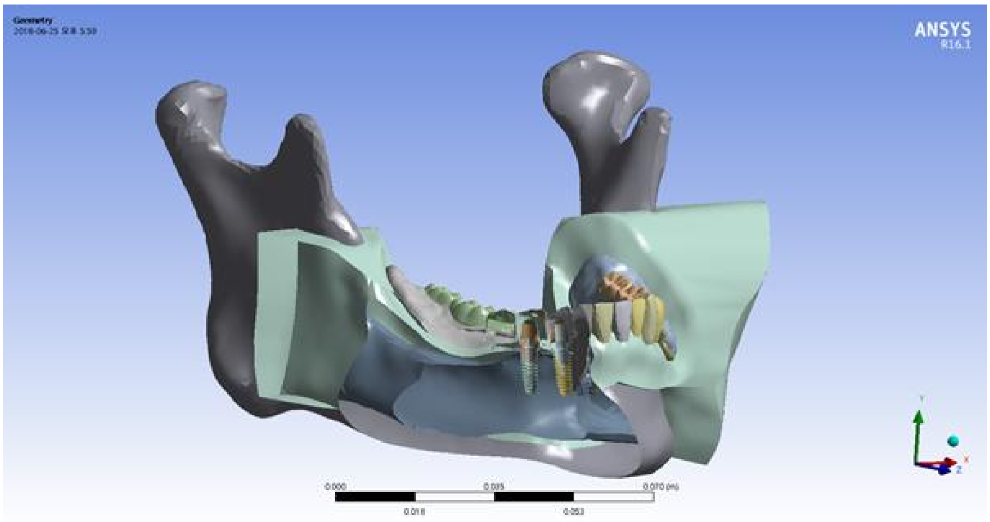

D.

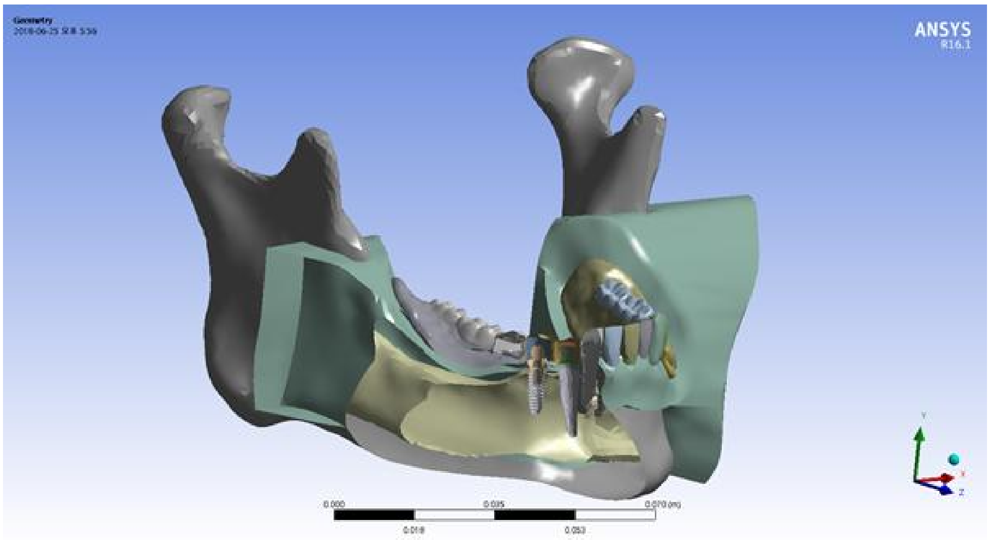

Fig. 2. A, Oblique occlusal loading site and direction B, Attachment sites of masticatory muscles

A

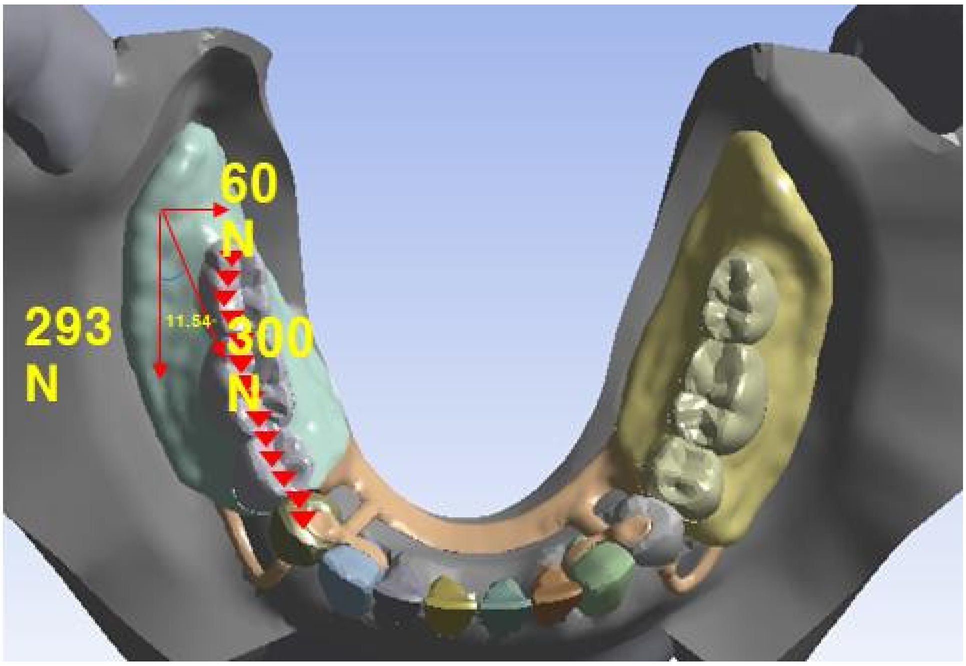

B

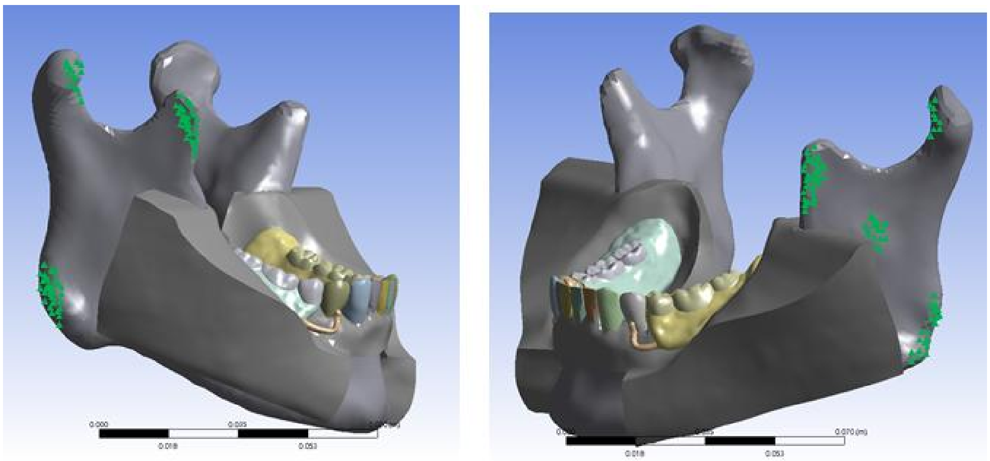

Fig. 3. The highest von Mises stress (GPa) of finite element models. A, Maximum von Mises stress of model 4TT. B, Maximum von Mises stress of model 4IT. C, Maximum von Mises stress of model 2IT.

A

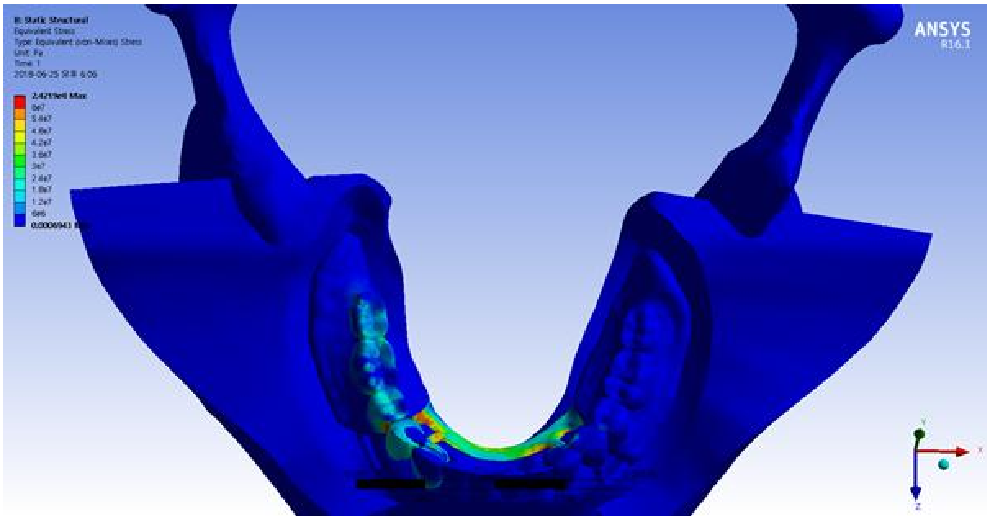

B

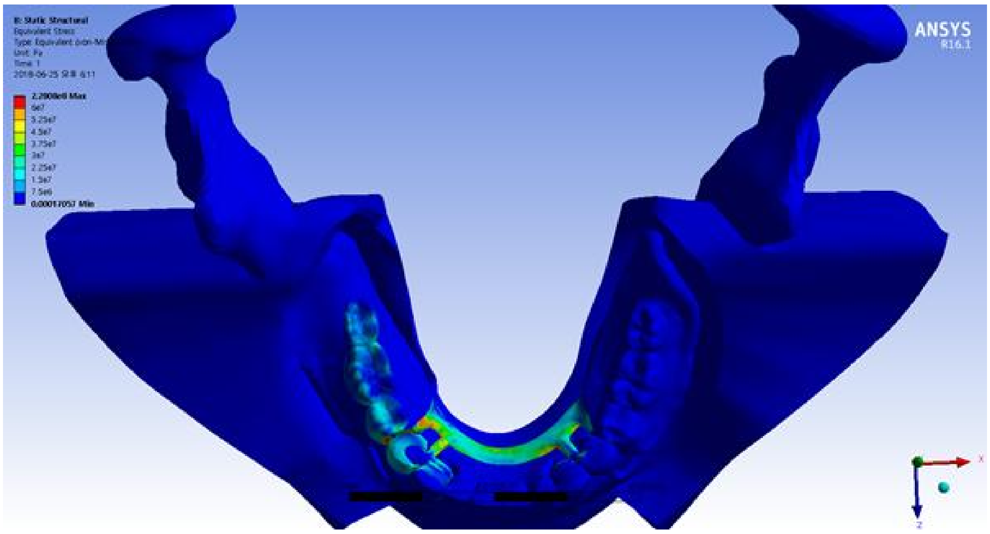

C

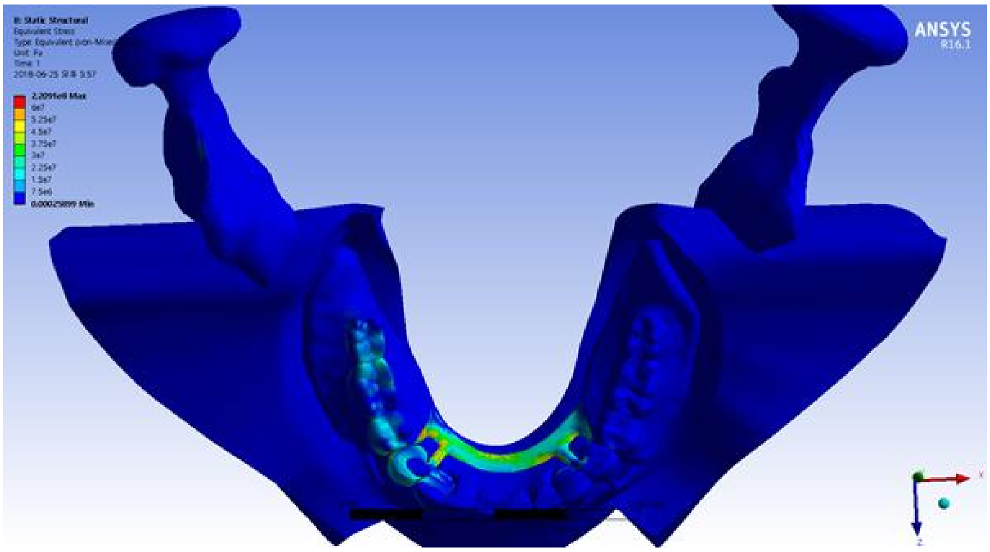
B: Static Structural
Equivalent Stress
Unit: Pa
Time: 1
6e7
5.25e7
4.5e7
3.75e7
3e7
2.25e7
1.5e7
7.5e6
ANSYS
R16.1

Fig. 4. The highest von Mises stress (GPa) of cortical bone.
A, Maximum von Mises stress of cortical bone of model 4TT.
B, Maximum von Mises stress of cortical bone of model 4IT.
C, Maximum von Mises stress of cortical bone of model 2IT.

A

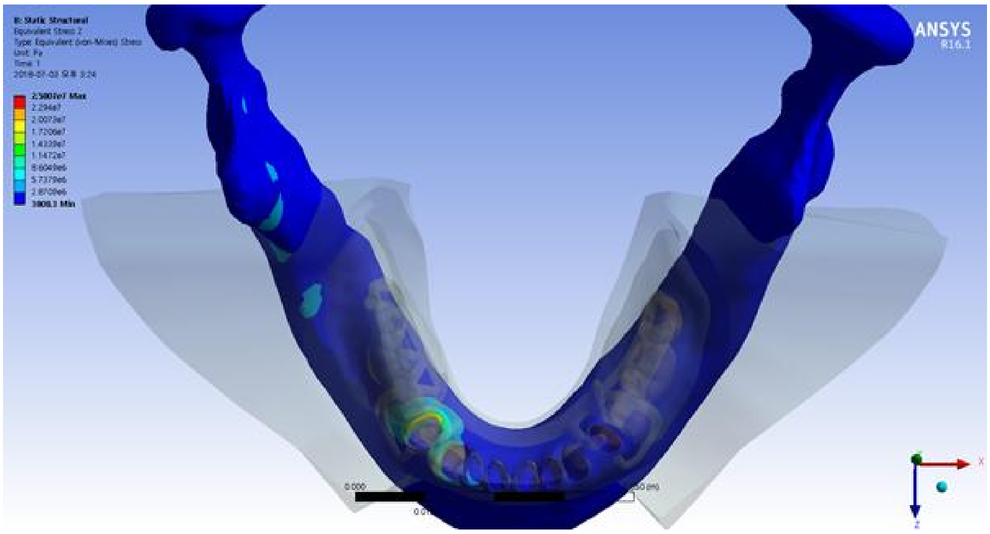

B

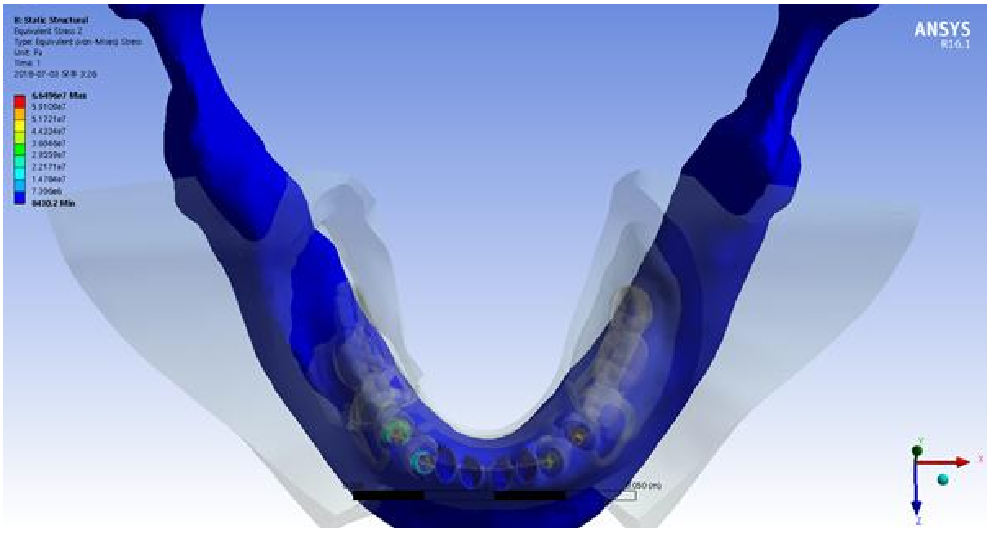

C

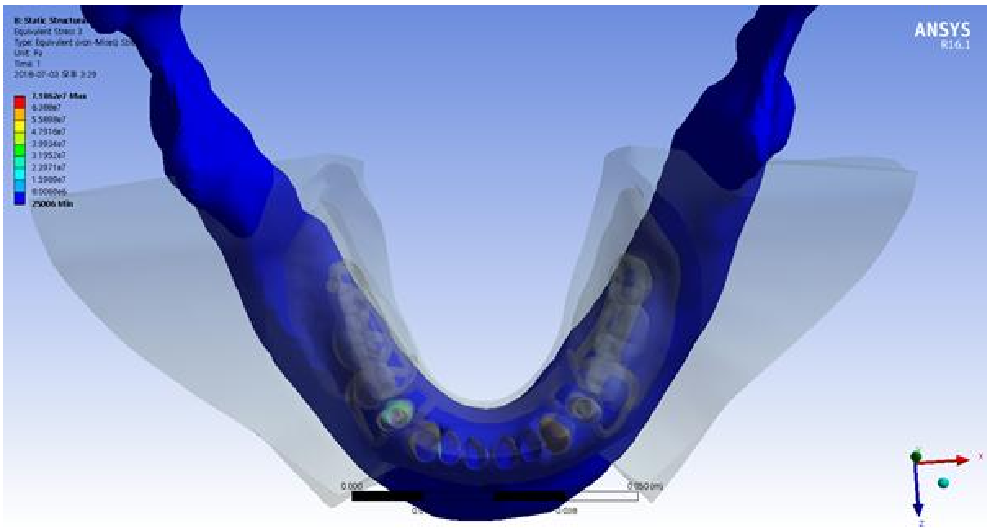

Fig. 5. The highest von Mises stress (GPa) of cancellous bone.
A, Maximum von Mises stress of cancellous bone of model 4TT.
B, Maximum von Mises stress of cancellous bone of model 4IT.
C, Maximum von Mises stress of cancellous bone of model 2IT.

A

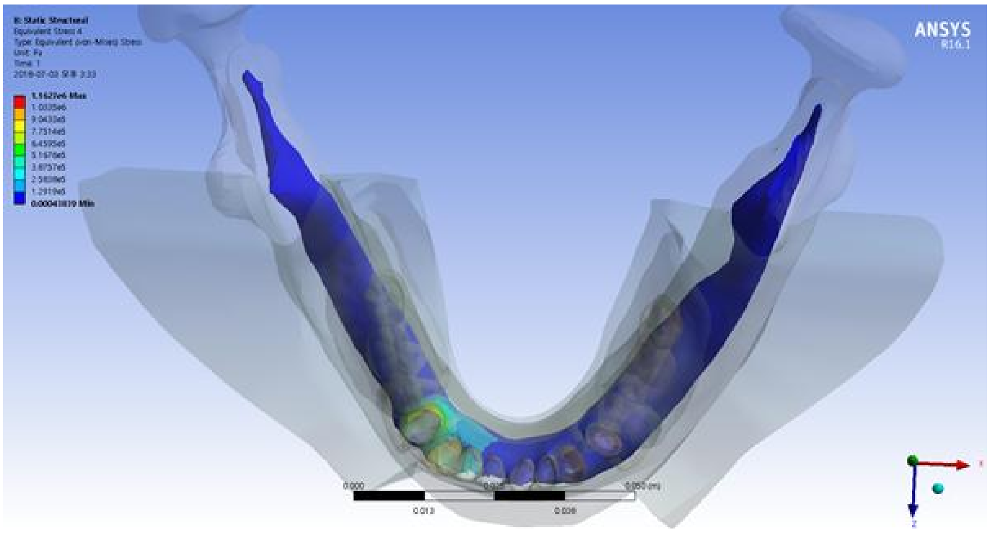

B

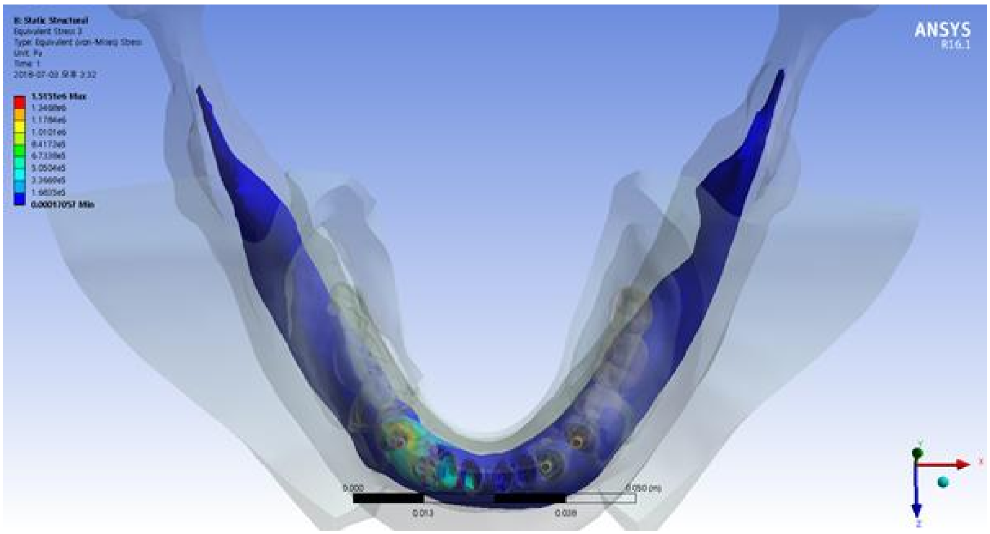

C

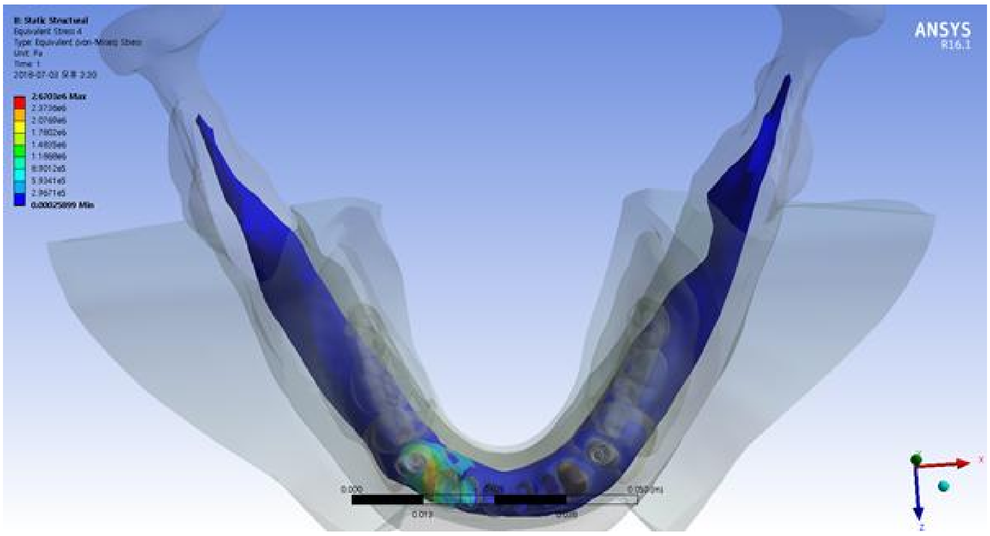

Fig. 6. The highest von Mises stress (GPa) of framework.
A, Maximum von Mises stress of framework of model 4TT.
B, Maximum von Mises stress of framework of model 4IT.
C, Maximum von Mises stress of framework of model 2IT.

A

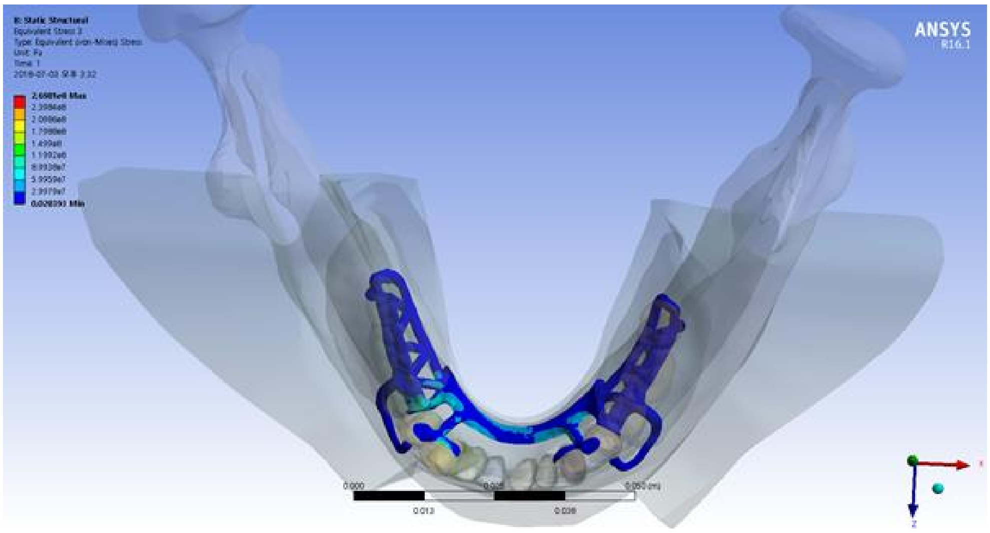

B

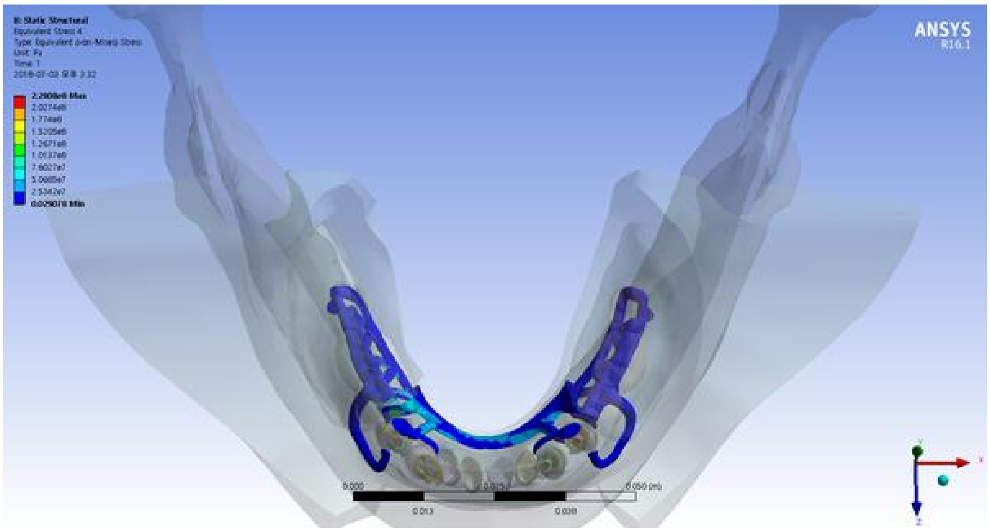

C

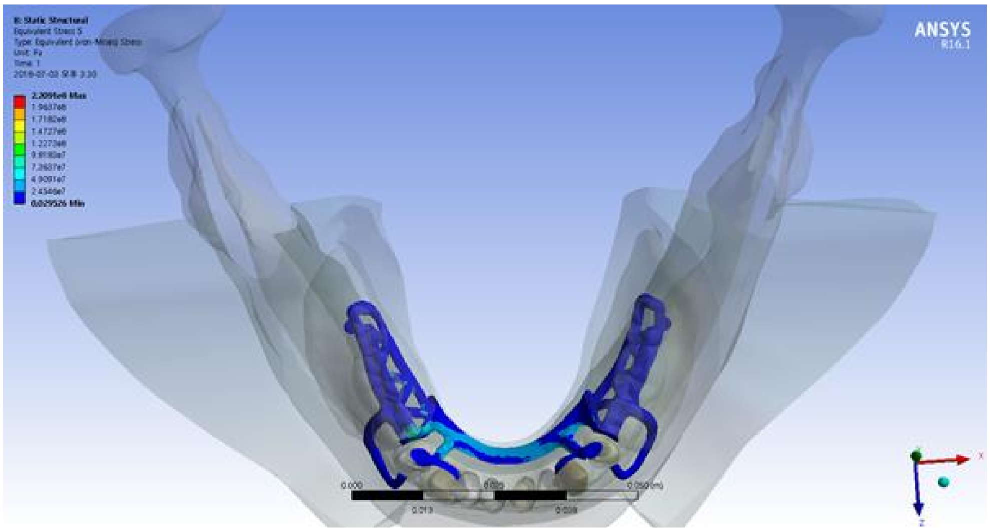
B: Static Structural
Equivalent Stress 5
Type: Equivalent (von-Mises) Stress
Unit: Pa
Time: 1
2.2091e8 Max
1.9637e8
1.7182e8
1.4727e8
1.2273e8
9.8180e7
7.3637e7
4.9091e7
2.4546e7
0.029526 Min
ANSYS
R16.1
0.000
0.050 (m)
X
Z

Fig. 7. The highest von Mises stress (GPa) of implant. A, Maximum von Mises stress of implant of model 4IT. B, Maximum von Mises stress of implant of model 2IT.

A

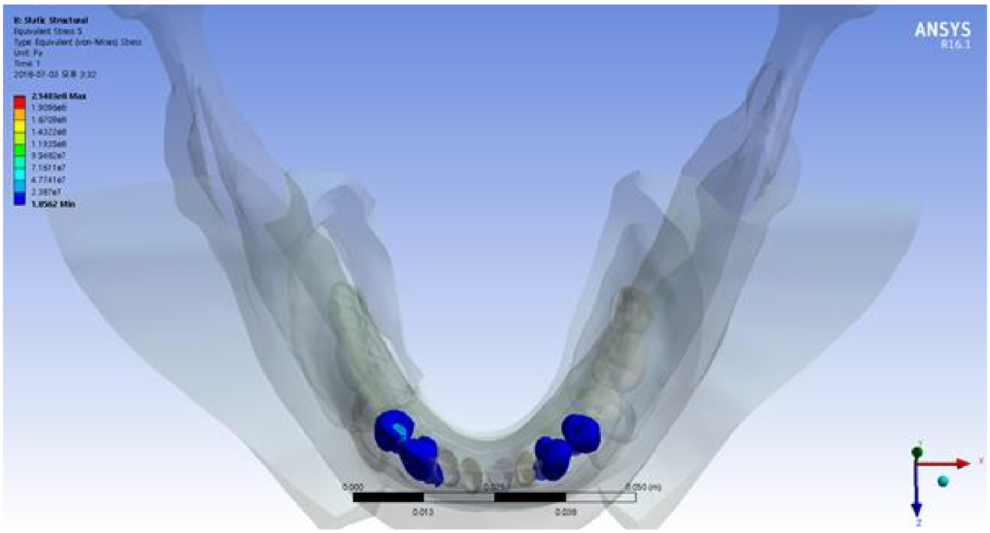

B

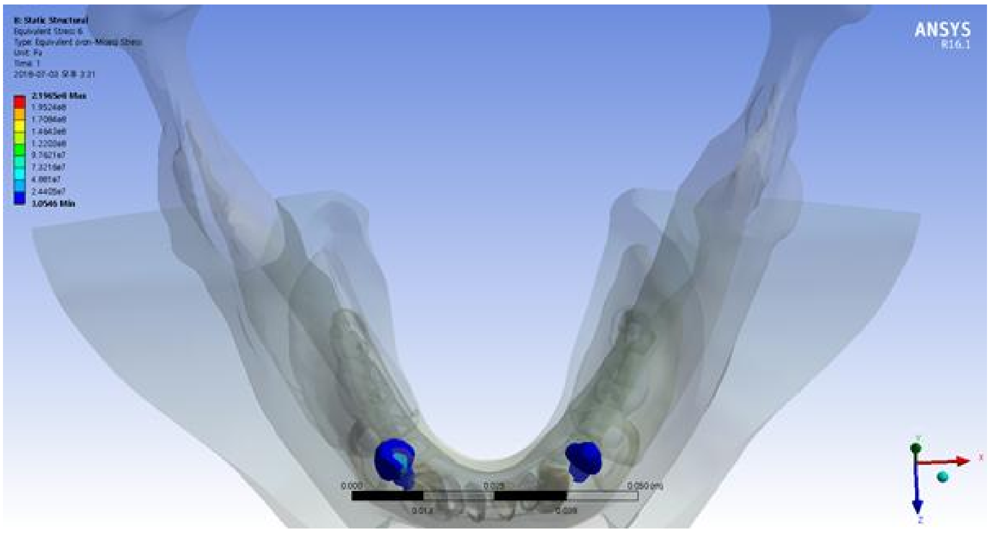

Fig. 8. Maximum displacement of finite element models. A, Maximum displacement of model 4TT. B, Maximum displacement of model 4IT. C, Maximum displacement of model 2IT.

A

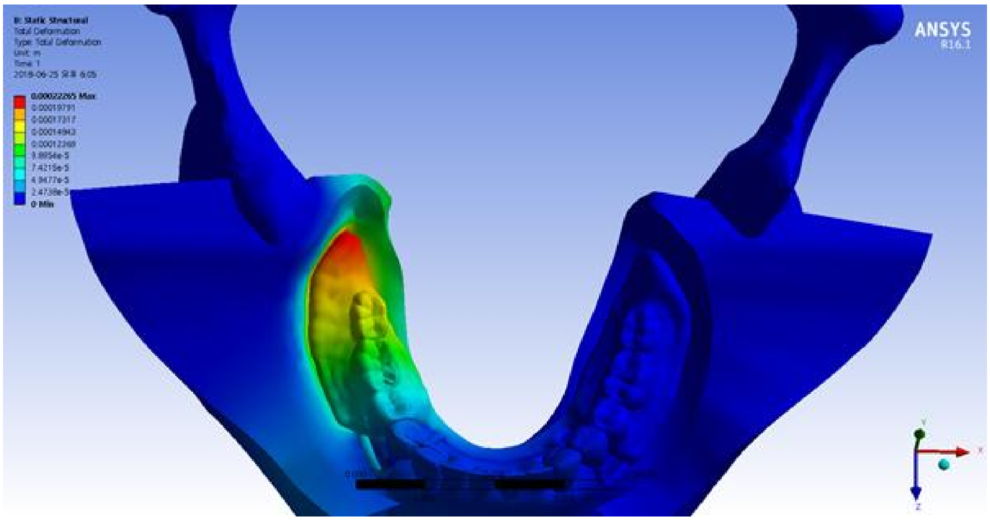

B

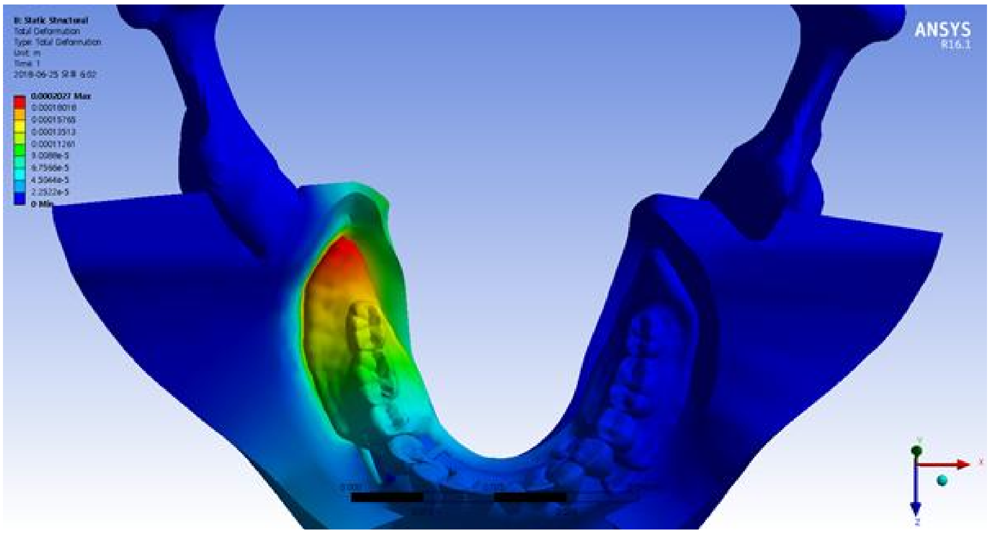

C

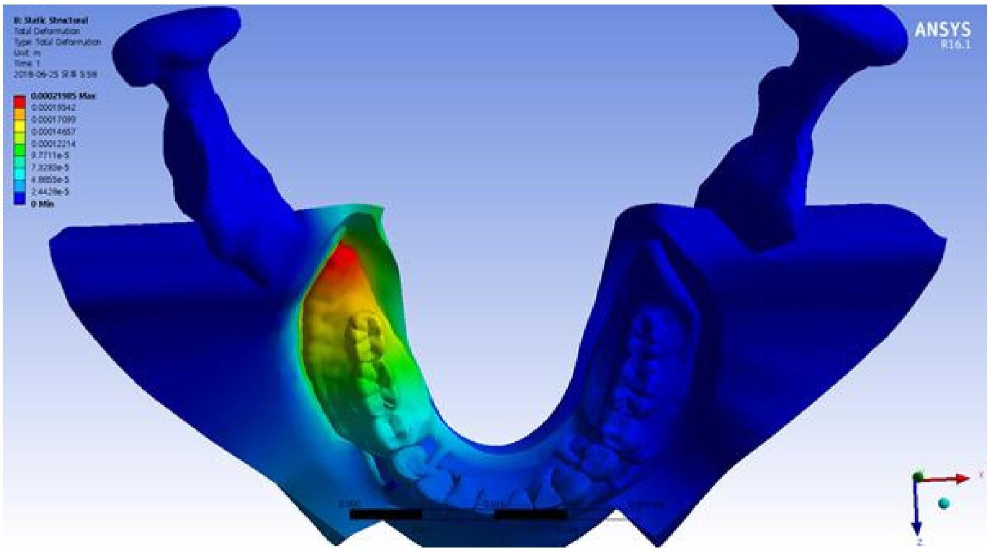
B: Static Structural
Total Deformation
Type: Total Deformation
Unit: m
Time: 1
0.00021985 Max
0.00019542
0.00017099
0.00014657
0.00012214
9.7711e-5
7.3283e-5
4.8855e-5
2.4428e-5
0 Min
ANSYS
R16.1
X
Z

References

Anitua, E., R. Tapia, F. Luzuriaga, and G. Orive. Influence of implant length, diameter, and geometry on stress distribution: a finite element analysis. *Int J Periodontics Restorative Dent.* 2010; 30: 89-95.

Bae, E. B., S. J. Kim, J. W. Choi, Y. C. Jeon, C. M. Jeong, M. J. Yun, S. H. Lee, and J. B. Huh. A Clinical Retrospective Study of Distal Extension Removable Partial Denture with Implant Surveyed Bridge or Stud Type Attachment. *Biomed Res Int.* 2017

Baggi, L., I. Cappelloni, M. Di Girolamo, F. Maceri, and G. Vairo. The influence of implant diameter and length on stress distribution of osseointegrated implants related to crestal bone geometry: a three-dimensional finite element analysis. *J Prosthet Dent.* 2008; 100: 422-31.

Bergman, B. Periodontal reactions related to removable partial dentures: a literature review. *J Prosthet Dent.* 1987; 58: 454-8.

Bergman, B., A. Hugoson, and C. O. Olsson. Caries, periodontal and prosthetic findings in patients with removable partial dentures: a ten-year longitudinal study. *J Prosthet Dent.* 1982; 48: 506-14.

Bergman, B., A. Hugoson, and C. O. Olsson. A 25 year longitudinal study of patients treated with removable partial dentures, *J Oral Rehabil*, 1995; 22: 595-9.

Budtz-Jorgensen, E., G. Bochet, M. Grundman, and S. Borgis. Aesthetic considerations for the treatment of partially edentulous patients with removable dentures. *Pract Periodontics Aesthet Dent.* 2000; 12: 765-72 de Carvalho, W. R., E. P. Barboza, and A. L. Caula. Implant-retained removable prosthesis with ball attachments in partially edentulous maxilla, *Implant Dent.* 2001; 10: 280-4.

Eom, J. W., Y. J. Lim, M. J. Kim, and H. B. Kwon. Three-dimensional finite element analysis of implant-assisted removable partial dentures. *J Prosthet Dent.* 2017; 117: 735-42.

Frank, R. P., J. S. Brudvik, and J. I. Nicholls. A comparison of the flexibility of wrought wire and cast circumferential clasps. *J Prosthet Dent.* 1983; 49: 471-6.

Ganz, S. D. Combination natural tooth and implant-borne removable partial denture: a clinical report. *J Prosthet Dent.* 1991; 66: 1-5.

Geng, J. P., K. B. Tan, and G. R. Liu. Application of finite element analysis in implant dentistry: a review of the literature. *J Prosthet Dent.* 2001; 85: 585-98.

Halterman, S. M., J. A. Rivers, J. D. Keith, and D. R. Nelson. Implant support for removable partial overdentures: a case report. *Implant Dent.* 1999; 8: 74-8.

Himmlova, L., T. Dostalova, A. Kacovsky, and S. Konvickova. Influence of implant length and diameter on stress distribution: a finite element analysis. *J Prosthet Dent.* 2004; 91: 20-5.

Jang, Y., S. Emtiaz, and D. P. Tarnow. Single implant-supported crown used as an abutment for a removable cast partial denture: a case report. *Implant Dent.* 1998. 7: 199-204.

Keith, O., R. P. Kusy, and J. Q. Whitley. Zirconia brackets: an evaluation of morphology and coefficients of friction. *Am J Orthod Dentofacial Orthop.* 1994; 106: 605-14.

Keltjens, H. M., A. F. Kayser, R. Hertel, and P. G. Battistuzzi. Distal extension removable partial dentures supported by implants and residual teeth: considerations and case reports. *Int J Oral Maxillofac Implants.* 1993; 8: 208-13.

Kim, Y., T. J. Oh, C. E. Misch, and H. L. Wang. Occlusal considerations in implant therapy: clinical guidelines with biomechanical rationale. *Clin Oral Implants Res.* 2005; 16: 26-35.

Kojima, Y., T. Mizuno, and H. Fukui. A numerical simulation of tooth movement produced by molar uprighting spring. *Am J Orthod Dentofacial Orthop.* 2007; 132: 630-8.

Lang, L. A., B. Kang, R. F. Wang, and B. R. Lang. Finite element analysis to determine implant preload. *J Prosthet Dent.* 2003; 90: 539-46.

Mericske-Stern, R., P. Assal, E. Mericske, and W. Burgin. Occlusal force and oral tactile sensibility measured in partially edentulous patients with ITI implants. *Int J Oral Maxillofac Implants.* 1995; 10: 345-53.

Mijiritsky, E. Implants in conjunction with removable partial dentures: a literature review. *Implant Dent.* 2007; 16: 146-54.

Mitrani, R., J. S. Brudvik, and K. M. Phillips. Posterior implants for distal extension removable prostheses: a retrospective study. *Int J Periodontics Restorative Dent.* 2003; 23: 353-9.

Montgomery, Jerome. Methods for modeling bolts in the bolted joint. In *ANSYS User's Conference*. 2002.

Murakami, N., and N. Wakabayashi. Finite element contact analysis as a critical technique in dental biomechanics: a review. *J Prosthodont Res.* 2014; 58: 92-101.

O'Mahony, A. M., J. L. Williams, and P. Spencer. Anisotropic elasticity of cortical and cancellous bone in the posterior mandible increases peri-implant stress and strain under oblique loading. *Clin Oral Implants Res.* 2001; 12: 648-57.

Ohkubo, C., M. Kobayashi, Y. Suzuki, and T. Hosoi. Effect of implant support on distal-extension removable partial dentures: in vivo assessment. *Int J Oral Maxillofac Implants.* 2008; 23: 1095-101.

Patterson, E. A., and R. B. Johns. Theoretical analysis of the fatigue life of fixture screws in osseointegrated dental implants. *Int J Oral Maxillofac Implants.* 1992; 7: 26-33.

Pellecchia, M., R. Pellecchia, and S. Emtiaz. Distal extension mandibular removable partial denture connected to an anterior fixed implant-supported prosthesis: a clinical report. *J Prosthet Dent.* 2000; 83: 607-12.

Pellizzer, E. P., F. R. Verri, R. M. Falcon-Antenucci, M. C. Goiato, and H. Gennari Filho. Evaluation of different retention systems on a distal extension removable partial denture associated with an osseointegrated implant. *J Craniofac Surg.* 2010; 21: 727-34.

Shahmiri, R. A., and M. A. Atieh. Mandibular Kennedy Class I implant-tooth-borne removable partial denture: a systematic review. *J Oral Rehabil.* 2010; 37: 225-34.

Shahmiri, R., J. M. Aarts, V. Bennani, M. A. Atieh, and M. V. Swain. Finite element analysis of an implant-assisted removable partial denture. *J Prosthodont.* 2013a; 22: 550-55.

Shahmiri, R., R. Das, J. M. Aarts, and V. Bennani. Finite element analysis of an implant-assisted removable partial denture during bilateral loading: occlusal rests position. *J Prosthet Dent.* 2014; 112: 1126-33.

Starr, N. L. The distal extension case: an alternative restorative design for implant prosthetics. *Int J Periodontics Restorative Dent.* 2001; 21: 61-7.

Van Staden, R. C., H. Guan, and Y. C. Loo. Application of the finite element method in dental implant research. *Comput Methods Biomech Biomed Engin.* 2006; 9: 257-70.

Wang, H. Y., Y. M. Zhang, D. Yao, and J. H. Chen. Effects of rigid and nonrigid extracoronal attachments on supporting tissues in extension base partial removable dental prostheses: a nonlinear finite element study. *J Prosthet Dent.* 2011; 105: 338-46.

Werbitt, M. J., and P. V. Goldberg. The immediate implant: bone preservation and bone regeneration. *Int J Periodontics Restorative Dent.* 1992; 12: 206-17.

Wismeijer, D., A. Tawse-Smith, and A. G. Payne. Multicentre prospective evaluation of implant-assisted mandibular bilateral distal extension removable partial dentures: patient satisfaction. *Clin Oral Implants Res.* 2013; 24: 20-7.

Yeung, S., W. W. Chee, and A. Torbati. Design concepts of a removable partial dental prosthesis with implant-supported abutments. *J Prosthet Dent.* 2014; 112: 99-103.

-국문초록-

하악 후방연장 임플란트-보조 가철성 국소의치의 삼차원 유한요소분석

서울대학교 대학원
치의과학과 치과보철학 전공

(지도교수 권 호 범)

엄 주 원

목 적 : 이 연구의 목적은 3차원 유한요소법을 이용하여 2가지 종류의 임플란트를 지대치로 한 하악 후방연장 임플란트-보조 가철성 국소의치와 자연치를 지대치로 한 가철성 국소의치의 생역학적 양상을 비교분석하여, 임플란트-보조 가철성 국소의치에서의 임플란트가 가철성 국소의치의 지대치로서의 기능을 할 수 있는지 평가한다.

재료 및 방법 : 환자의 CT 영상으로부터 하악골 유한요소 모델을 만들고, 써베이 크라운, 치아 및 삼차원 모델링 후방연장 국소의치 임플란트와 함께 서로 다른 형태의 세가지 하악 후방연장 가철성 국소의치 모델을 만들었다.

써베이 크라운 및 가철성 국소의치 모델은 삼차원 모델링 프로그램으

로 (Visual-Mesh; ESI group) 모델링 하였고, 가철성 국소의치 모형은 금속구조물, 아크릴 레진상 및 의치로 구성되어져 있다. 임플란트는 직경 4mm, 길이 10mm인 내측연결형 임플란트 (Osstem GS system; Osstem Implant Co) 를 사용하였고, 치아 교합면에 협측에서 설측으로 300 N의 사선방향의 힘을 상부 크라운 및 국소의치 치아에 가한 후, 각각의 구성요소에 가해지는 등가응력 (von Mises stress) 과 전체 모델의 움직임 양을 조사하였다.

결 과 : 세 가지 모델 중 자연치 모델 (4TT) 에서 가장 높은 응력값 (242.2 MPa) 이 관찰되었다. 세 가지 모델 모두 가장 높은 응력값은 국소의치의 금속구조물의 부연결장치에서 관찰되었다. 네개의 임플란트-보조 국소의치 (4IT) 에서의 가장 높은 응력값 (228.1 MPa) 은 두개의 임플란트-보조 국소의치 (2IT) 에서보다 약간 더 높은 값 (220.9 MPa) 을 보였다. 임플란트-보조 국소의치에서 두 번째로 높은 응력값을 지진 구조물은 임플란트 지대주였다. 4개의 임플란트-보조 국소의치(4IT)의 임플란트에서의 가장 높은 응력값 (214.8 MPa) 은 2개의 임플란트-보조 국소의치 (2IT) 에서의 임플란트에서 (219.7 MPa) 보다 약간 더 낮은 값 을 보였다. 세 개의 모델중 치아지지 국소의치 (4TT) 에서 가장 높은 변위량 (0.2265 mm) 을 보였고, 2개의 임플란트-보조 국소의치 (2IT) 에서 그다음 변위량 (0.2199 mm) 을 보였으며, 4개의 임플란트-보조 국소의치 (4IT) 에서 변위량 (0.2027 mm) 은 가장 작았다. 세 개의 모델 모두에서 변위량은 국소의치 가장 원심 후방부위의 아크릴릭 레진상에서 가장 컸다.

결 론 : 임플란트-보조 가철성 국소의치에서 가장 큰 등가응력은 국소의치의 금속구조물에서 보였고, 두번째로 높은 등가응력은 임플란트 지대주에서 보였다. 임플란트-보조 국소의치에서 임플란트 지대치의 개수가 많을수록 임플란트에 가해지는 등가응력의 크기는 줄어들었다. 자

연치를 지대치로 한 전통적인 가철성 국소의치와 두종류의 임플란트-보조 국소의치에서의 최대 등가응력값과 최대 움직임양의 큰 차이는 없었다. 하악후방연장 임플란트-보조 가철성 국소의치를 제작할 때 임플란트에 가해지는 응력을 줄일 수 있도록 설계가 된다면, 임플란트를 지대치로 한 임플란트-보조 가철성 국소의치는 부분무치악 환자에서 보다 편안하고, 만족스러운 치료방법이 될 수 있다.

주요어 : 치과용 임플란트, 임플란트-보조 국소의치, 임플란트-융합 국소의치, 임플란트-지지 국소의치, 하악 후방연장 가철성 국소의치, 유한요소분석

학 번 : 2011-31182